The Partitioning of Phosphoramide Mustard and Its Aziridinium Ions among Alkylation and P−N Bond Hydrolysis Reactions

Ellen M. Shulman-Roskes,[†] Dennis A. Noe,[†] Michael P. Gamcsik,[‡] Allison L. Marlow,[†] John Hilton,[†] Frederick H. Hausheer,[§] O. Michael Colvin,[‡] and Susan M. Ludeman*[,‡]

The Johns Hopkins University School of Medicine, Baltimore, Maryland 21287, BioNumerik Pharmaceuticals, Inc., San Antonio, Texas 78229, and Duke University Department of Medicine, Durham, North Carolina 27710

Received July 16, 1997

NMR (^{1}H and ^{31}P) and HPLC techniques were used to study the partitioning of phosphoramide mustard (PM) and its aziridinium ions among alkylation and P−N bond hydrolysis reactions as a function of the concentration and strength of added nucleophiles at 37 °C and pH 7.4. With water as the nucleophile, bisalkylation accounted for only 10−13% of the product distribution given by PM. The remainder of the products resulted from P−N bond hydrolysis reactions. With 50 mM thiosulfate or 55−110 mM glutathione (GSH), bisalkylation by a strong nucleophile increased to 55−76%. The rest of the PM was lost to either HOH alkylation or P−N bond hydrolysis reactions. Strong experimental and theoretical evidence was obtained to support the hypothesis that the P−N bond scission observed at neutral pH does *not* occur in the parent PM to produce nornitrogen mustard; rather it is an aziridinium ion derived from PM which undergoes P−N bond hydrolysis to give chloroethylaziridine. In every buffer studied (bis-Tris, lutidine, triethanolamine, and Tris), the decomposition of PM (with and without GSH) gave rise to ^{31}P NMR signals which could not be attributed to products of HOH or GSH alkylation or P−N bond hydrolysis. The intensities of these unidentified signals were dependent on the concentration of buffer.

Introduction

For any anticancer agent, there is generally one pathway which leads to a therapeutic response. Deviations from this pathway are often important contributors to other effects such as detoxification and drug resistance. Factors which govern the mechanistic fate of a drug are complex, but they generally can be explained, at least in part, through considerations of molecular structure. Such is the case for cyclophosphamide (CP) and its metabolites.

Oxidative activation of the prodrug cyclophosphamide leads to a cascade of metabolites, ultimately resulting in what is generally accepted as the alkylating agent of therapeutic consequence, phosphoramide mustard (PM).[1−3] The work reported herein began as an investigation of reactions which might occur spontaneously between PM and the tripeptide glutathione (GSH). Alkylation of GSH by PM would represent an irreversible detoxification and a possible mechanism of resistance in cells with elevated levels of GSH.[4,5] At one time, such reactions were reported not to occur in the absence of enzymatic assistance;[6] subsequently, and concurrent with this work, others showed that such reactions did not require enzymatic intervention.[7] Our work supports the spontaneous nature of the reaction and broadens the reported work by providing a more extensive quantification of the reactions available to PM.

For the first time, it was demonstrated that nucleophile strength and concentration impact on the distribution of products given by PM. It was also shown that the incidence of a competing P−N bond hydrolysis reaction *at neutral pH* is a significant issue in the chemistry of PM. It has long been assumed that a P−N bond hydrolysis pathway for PM would result in the formation of nornitrogen mustard (NNM), and apparently, such is the case under acidic conditions (pH < ca. 4.5).[8−10] In this study, experimental (NMR) as well as theoretical (quantum chemical calculations) data were obtained which demonstrate that P−N bond scission occurs under neutral conditions. Most notably, the evidence also supports the conclusion that this P−N bond hydrolysis does *not* occur in the parent molecule to produce NNM. Rather it is the aziridinium ion formed from PM which hydrolyzes to give the bisalkylating agent *chloroethylaziridine* (CEZ). Concurrent with our first proposal of this pathway,[11] the same reaction was suggested by Lu and Chan when they detected CEZ but not NNM in buffered solutions of PM.[12] These authors also stated, however, that conversion of NNM to CEZ was a facile process at pH 7.4, and they did not appear to rule out the intermediacy of NNM in CEZ formation.

There is much data in the literature (by us and others) to support the conclusion that the half-life of the parent PM is independent of buffer-type.[9,10,13] The studies reported herein, however, reveal that PM can give a product array which is very buffer-dependent. In every buffer studied (bis-Tris, lutidine, triethanolamine, and Tris), ^{31}P NMR signals were observed which could not be attributed to products of GSH or HOH alkylation or P−N bond hydrolysis.

* To whom correspondence should be addressed at Duke Comprehensive Cancer Center, Box 3843, Duke University Medical Center, Durham, NC 27710.
[†] Johns Hopkins University.
[‡] Duke University.
[§] BioNumerik Pharmaceuticals.

S0022-2623(97)00465-2 CCC: $15.00
Published on Web 01/17/1998

We now report NMR and HPLC investigations of PM (**1**) and the partitioning of its aziridinium ions (**2**, **4**, and **9**) among spontaneous alkylation and P−N bond hydrolysis reactions as a function of nucleophile strength and concentration.

Results and Discussion

Theoretical Studies of Aziridinium Ion Structure. Prior to the beginning of our experimental work, the susceptibility of PM aziridinium ions toward hydrolysis of the $P-N^+$ bond was predicted by ab initio quantum chemical calculations. Using a 6-31G* basis set, Hartree−Fock (HF)[14−16] optimized, gas phase, equilibrium structures were calculated for ethyl analogues of PM and its aziridinium ions. The calculated bond lengths (Å) are shown below. At the time of this analysis, the ethyl analogues were used to reduce the complexity of the calculations. Reported after this analysis were similar calculations (6-31G* HF-optimized[16]) for PM.[17] The good agreement between the results for PM (also shown below) and its diethyl congener support the reliability of the ethyl analogues as models.

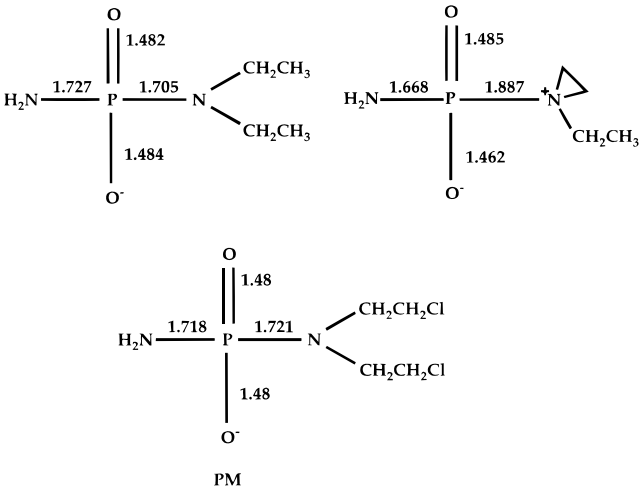

PM

On the basis of these calculations for the models, formation of an aziridinium ion increases the bond length between phosphorus and the aziridinyl nitrogen from 1.703 to 1.887 Å. By way of comparison, the anion of phosphoramidic diacid $[(H_3N^+)PO_3^{2-}]$ has been cited as having a "special place in P−N chemistry" because this ion is considered to have an authentic P−N single bond free of π contributions (bond length = 1.77 Å).[18] The P−N bond in the aziridinium model, therefore, would be predictably unstable due to its unusual length as well as its decreased π character. Notably, increased susceptibility to hydrolytic bond cleavage would be pH independent. This is in contrast to any P−N bond hydrolysis which might occur in PM itself, prior to aziridinium ion formation.[8]

Shown below are the bond angles calculated for the ethylaziridinium ion model in its HF-optimized, gas phase, equilibrium geometry. An examination of these angles reveals that the phosphorus atom, the two oxygens, and the nitrogen of the NH_2 group are nearly coplanar. As shown in the first illustration, the sum of the three bond angles made by these atoms is 350.3°. This value approaches the sum (360°) of the bond angles given by a similar array of atoms in a trigonal plane. The calculated bond angles shown in the second illustration indicate that the aziridinyl moiety is nearly perpendicular to the other three ligands. This geometry is very vulnerable to a hydrolysis mechanism wherein the aziridinyl moiety leaves from an apical position through a trigonal bipyramid transition state.

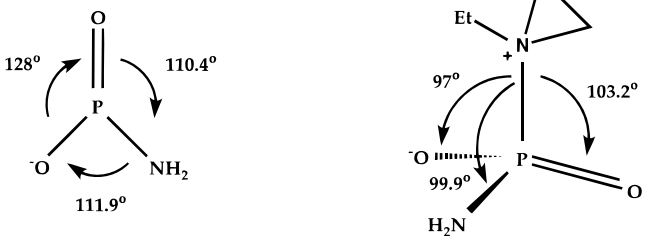

Although the equilibrium structures discussed above were determined for the gas phase, calculations of this type often give similar results for species in gas and solution phases.

Chloroethylaziridine (CEZ) Formation. Throughout the long-written record of CP chemistry, metabolic pathways which have included a P−N bond hydrolysis pathway for PM have shown nornitrogen mustard (NNM) as the product. The intramolecular cyclization of NNM might then account for the CEZ which has been reported as a CP metabolite.[12,19] As a result of the theoretical studies, however, we were prompted to question and to reinvestigate this traditional view. As a framework for our experimental studies, three pathways for CEZ formation were considered, as shown in Scheme 1. Path A reflects the traditional view. Path B is a variation on that and incorporates previously reported experimental and theoretical data showing that, under aqueous conditions, the nitrogen of the NH_2 moiety is more likely to become protonated than is the nitrogen of the mustard group (presumably a condition required for hydrolysis).[17,20] Path C represents a new proposal by us and others[11,12] which invokes P−N bond scission of the first aziridinium ion (**2**) formed from PM rather than bond cleavage in PM itself. In the following section, convincing experimental evidence is presented which, for the first time, supports pathway C as the primary route of CEZ formation at neutral pH.

NMR Studies of CEZ Formation. P−N bond hydrolysis in PM via path A, Scheme 1, was probed using ^1H NMR spectroscopy. For simplification of the proton spectra, PM was synthesized as the free acid rather than as the cyclohexylammonium salt. NMR samples were made with 0.05 M phosphate in D_2O at pD 7.4, and spectra were acquired at varying time points. As shown in Figure 1, separate resonances indicative of NNM (δ 3.84 and 3.32 at pD 7.4, 5 °C) could not be observed; however, it was possible that the NNM signals were overlapped by the multiplets arising from unreacted PM (δ 3.66 and 3.32) and/or hydroxylated, alkylation products. Thus, an aliquot of the PM reaction mixture was spiked with authentic NNM; spectral analysis of this sample revealed a well-resolved triplet at δ 3.84 for the CH_2Cl moiety of NNM where none had been detected previously (Figure 1). There were minor resonances in this region of the spectrum which were

Scheme 1

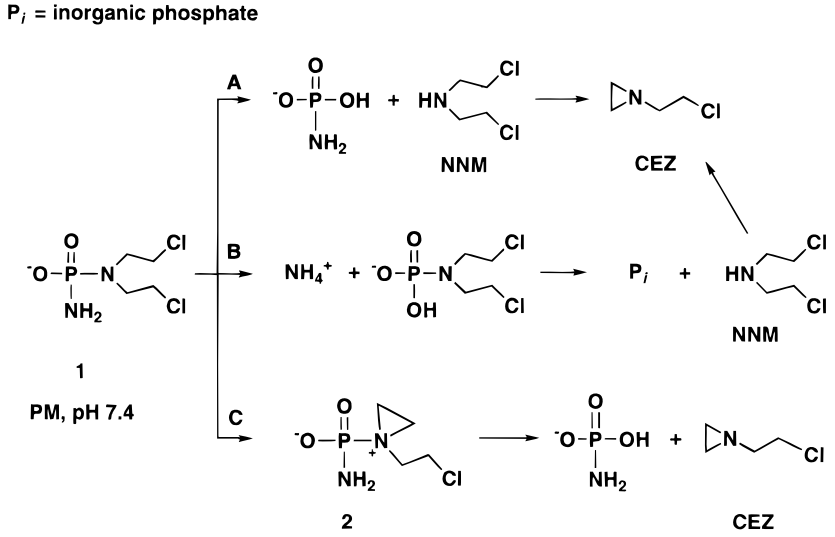

close but not identical with that for NNM. At one time, we erroneously attributed one of these signals to NNM.[21]

While NNM could not be detected in the reaction sample containing PM, unobscured signals assignable to CEZ were observed at δ 3.74 (t, CH_2Cl), 2.76 (t, CH_2N), and 1.98 and 1.66 (m, aziridinyl ring protons), as shown in Figure 1. Confirmation of the signal assignments was achieved through the use of authentic CEZ (see the Experimental Section).

Even though NNM was not detected in the NMR spectra, path A could not be ruled out as the source of CEZ. Because the kinetics of NNM formation and disappearance might be similar, it was possible that this compound was not detected in NMR samples of PM because the concentration of transient NNM was too low to be detected by ^{1}H NMR. To probe this, a simulation was carried out to determine what the NNM concentration might be if it were an intermediate. To simplify the situation of complex kinetics occurring through multiple pathways, some assumptions were made. The sequence PM → NNM → CEZ was assumed to occur through consecutive first-order reactions with CEZ being the "final" product. These assumptions were reasonable based on the facts that the relevant reactions would be first- or pseudo-first-order and that the stability of CEZ[12] was much greater than that of PM or NNM (vide infra). It was also assumed that the rate of formation of NNM could not be greater than the reported rate of PM disappearance ($\tau_{1/2}$ = 18 min, k = 0.038 min^{-1} at pH 7.4, 37 °C).[9,13] The rate constant for the disappearance of NNM was determined by ^{1}H NMR to be 0.0411 ± 0.0007 min^{-1} (n = 3) in 0.1 M phosphate in 5% D_2O, pH 7.4, 37 °C ($\tau_{1/2}$ = 17 min). This was in accord with the half-life for NNM reported by Lu and Chan, i.e., $\tau_{1/2}$ = 14.5 min in 0.067 M phosphate, pH 7.4, 37 °C.[12] Simulations[13] were run assuming a 10% conversion of PM to NNM; this was a very conservative estimate based on the ^{31}P data and kinetic analysis discussed later (i.e., in the absence of a good nucleophile, the primary fate of PM is participation in a sequence which at some point involves hydrolysis).

The results of the simulation showed that maximal NNM concentration would occur ca. 25 min after PM began to react and that this maximal concentration would be ca. 35% that of the "final" concentration of CEZ. Since CEZ was readily observed in the NMR spectra, these data suggested that if NNM were the precursor to CEZ, its formation in solution should have been detectable in an unambiguous manner. This conclusion was valid over a range of rate constants for NNM formation and disappearance, as pointed out by a reviewer of this manuscript. As shown in Figure 1, there was no resonance of the appropriate intensity for NNM at δ 3.84 in the spectrum representing t = 30 min.

These data provided arguments against the formation of NNM and, therefore, against significant contributions from path A and, necessarily, path B at neutral pH (Scheme 1). Additional evidence against path B was derived from ^{31}P NMR experiments. In reaction solutions of PM, two ^{31}P NMR signals were clearly visible in the chemical shift region associated with phosphate and phosphoramidic diacids (δ +5 to −5). Using authentic materials to spike a reaction solution at 37 °C, one of the resonances was ascribed to inorganic phosphate (δ 1.9, pH 7.4) and one to the phosphoramidic diacid[20] which would be formed via path A or C ($H_2N-PO_3H^-$: δ −1.0, pH 7.4). Authentic $(ClCH_2CH_2)_2N-PO_3H^-$ (which would be produced by path B) had a chemical shift (δ 4.6, pH 7.4) which did not match any reasonance visible in a time frame concurrent with CEZ formation. The chemistry of $(ClCH_2CH_2)_2N-PO_3H^-$ was not explored further, and it must be noted that, as with NNM, an inability to detect this species in the NMR spectra does not rule out its formation.

With doubts cast on paths A and B, formation of CEZ via path C was considered most likely, especially in view of the theoretical data discussed above. A simple consideration of the electronic structure of aziridinium ion **2** clearly indicated that the $P-N^+$ bond would be susceptible to cleavage. But perhaps the most compelling argument for the formation of CEZ from aziridinium ion **2** rather than from NNM was derived from an analysis of the ^{31}P NMR experiments discussed in a following section. These experiments demonstrated that the incidence of P−N bond scission in PM was dependent on the strength and concentration of added nucleophiles. Direct hydrolysis of PM to NNM would

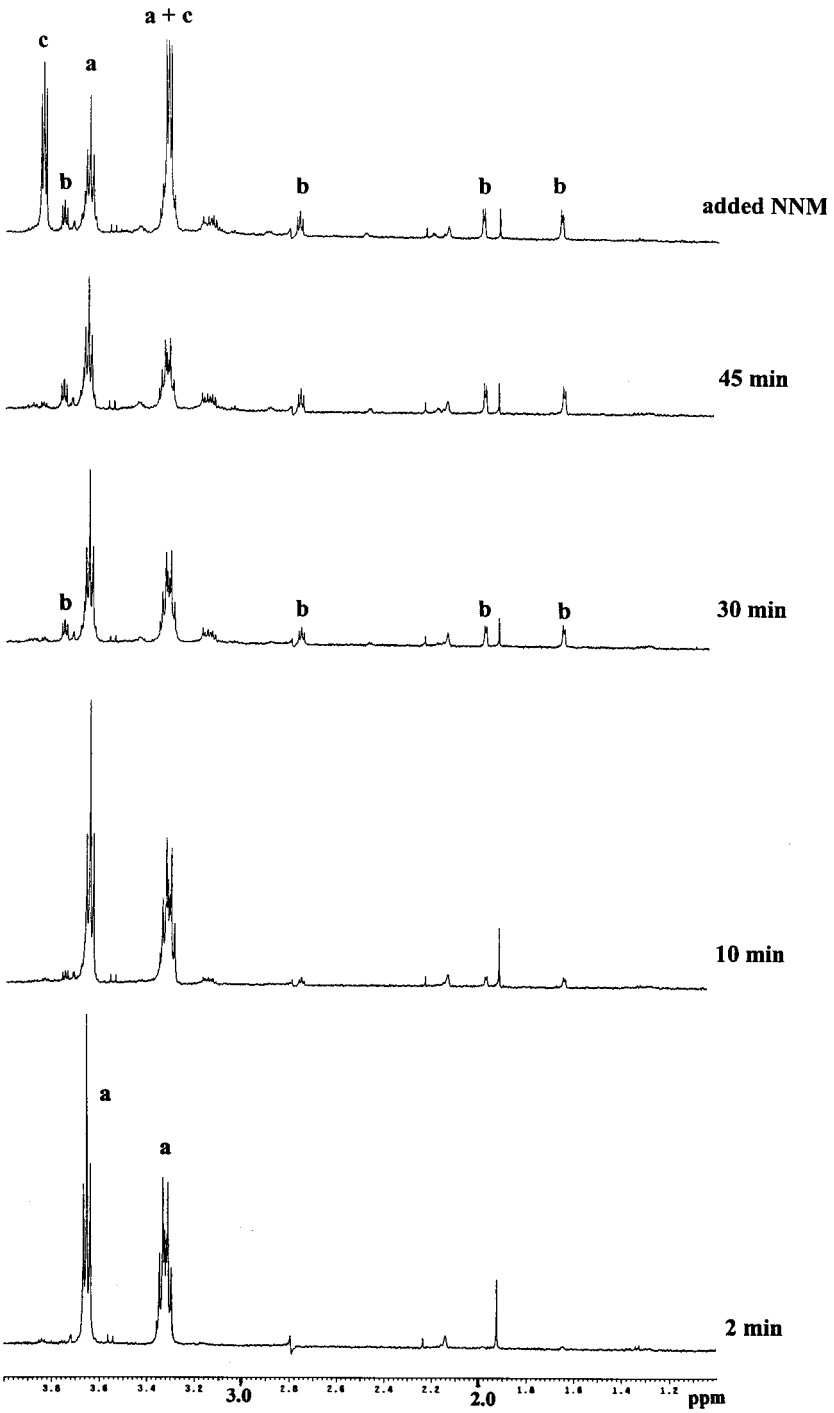

Figure 1. ^{1}H NMR (500 MHz) spectra showing the formation of CEZ in solutions of PM. Minutes refer to the time when aliquots were removed from a solution of PM in D_2O at 37 °C, pD 7.0−7.5. These aliquots were then added to 0.05 M phosphate in D_2O at pD 7.4 and spectra were obtained on these samples at 5 °C using internal TSP-d_4 as the chemical shift reference (see the Experimental Section for details). The top spectrum represents a sample at the 45 min time interval but with added NNM. Signal assignments: a = PM; b = CEZ; and c = NNM.

be a process uninfluenced by the presence of nucleophiles other than water.

CEZ Stability. A cursory examination of CEZ revealed that this compound was relatively stable under the conditions of the NMR experiment ($\tau_{1/2} \gg 5$ h in 0.1 M phosphate in D_2O, pD 7, 37 °C). This observation was consistent with the reported half-life for CEZ of 20 h in 0.067 M phosphate, pH 7.4, 37 °C.[12] We did determine the pK_a of CEZ to be 6.62 and are able to attribute the stability of the aziridinyl ring in this molecule, relative to that in **2** for example, to its being neutral at pH 7.4. This stability is, of course, dependent on the presence or absence of nucleophiles in solution. In the presence of excess GSH, the stability of CEZ dropped significantly: in 0.1 M phosphate in D_2O, pD 7 (initial) − 6.8 (final), 37 °C, the rate constant for the reaction of CEZ (1 mM) with GSH (10 mM) was 0.0130 min^{-1} ($\tau_{1/2}$ = 53 min). Because the pH of the solution in this experiment drifted, this rate value can only be viewed as an estimate.

Alkylation and P−N Bond Hydrolysis Reactions of Phosphoramide Mustard (PM). The complex set

Scheme 2

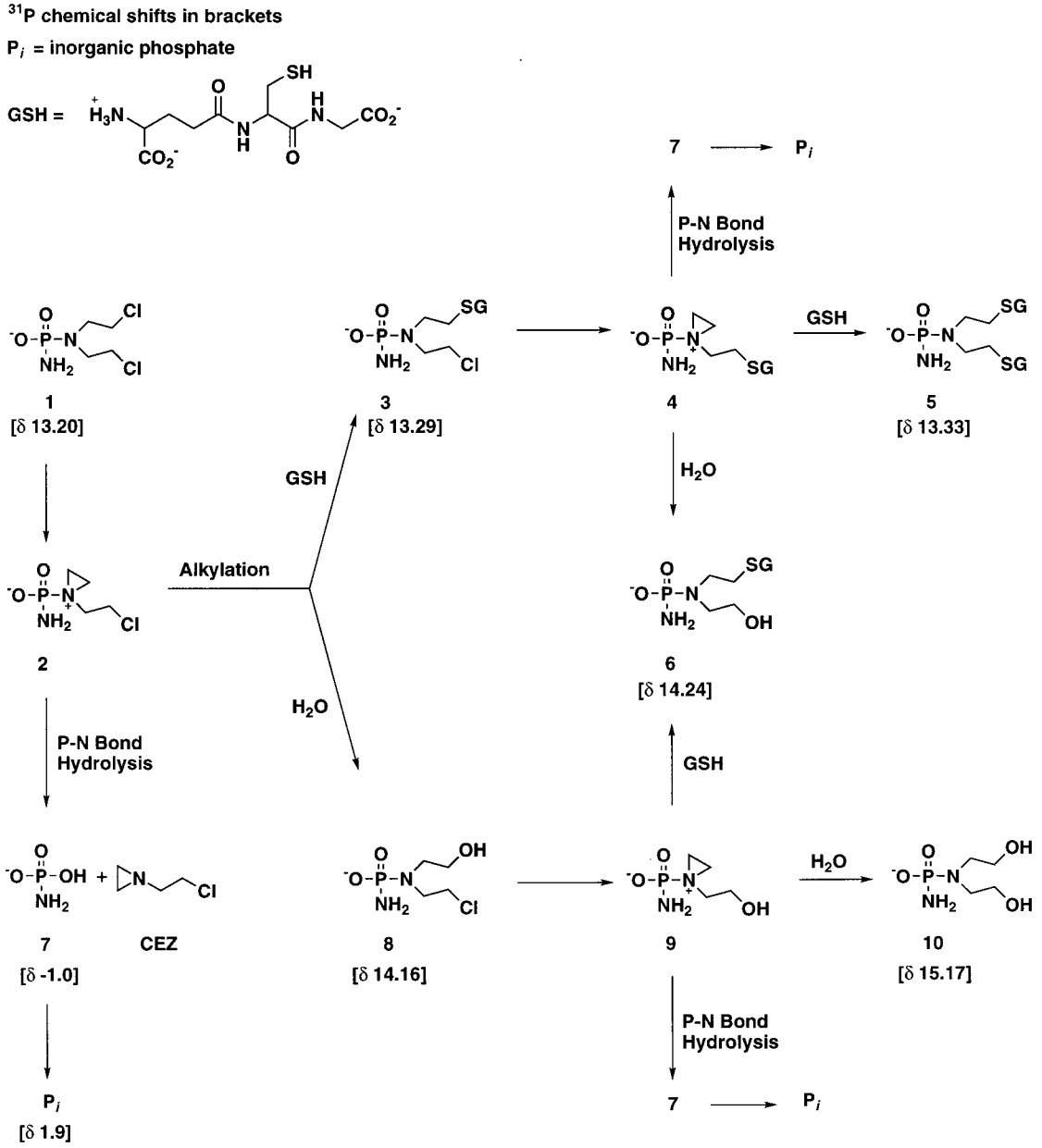

of spontaneous reactions available to PM (**1**) will be broadly characterized as alkylation and P−N bond hydrolysis reactions as illustrated in Scheme 2, where an aziridinium ion is the branch point for these competing pathways. Alkylation reactions will include the reaction of any nucleophile with an aziridinium ion (**2**, **4**, **9**) to give an acyclic product. That PM undergoes alkylation reactions through the intermediacy of such ions has been well documented.[22] In Scheme 2, these alkylation reactions are illustrated for GSH, which is a strong nucleophile, and for water, which is ubiquitous and representative of a weak nucleophile. The alkylation sequences are **2** → **3** → **5**; **2** → **8** → **10**; and **2** → **3**/**8** → **6**. P−N Bond hydrolysis reactions are those involving hydrolytic cleavage of the $P-N^+$ bond in an aziridinium ion to produce CEZ (or an analogue thereof) and phosphoramidic diacid (**2**/**4**/**9** → **7**). As concluded in a previous section, direct P−N bond scission of PM (or any nonaziridinium species) to give NNM or an NNM-like product is not significant at neutral pH and, therefore, is not included in the scheme for PM chemistry.

Maintaining the distinction between alkylation of water and P−N bond hydrolysis as defined here is vital to the clarity of the following discussion and in comparisons of this work with that of others. What is described here as the alkylation of water has been been termed by others as a hydrolysis reaction.[7,10,12]

^{31}P NMR Studies of PM Reactivity. Using ^{31}P NMR, the reactivity of PM (11 mM) was studied in the presence of zero, 11, 22, 55, and 110 mM GSH at 37 °C and pH 7.4 (0.22 M bis-Tris). Spectra were acquired every 3.5 min over the first 2 h of reaction time. A final spectrum was taken 8−21 h after the initial acquisition (and in at least one run under each set of conditions, a final spectrum was taken at $t \geq 17$ h).

Signal identifications were based on a number of considerations including: (a) use of authentic materials; (b) time frames for signal disappearance and/or growth;

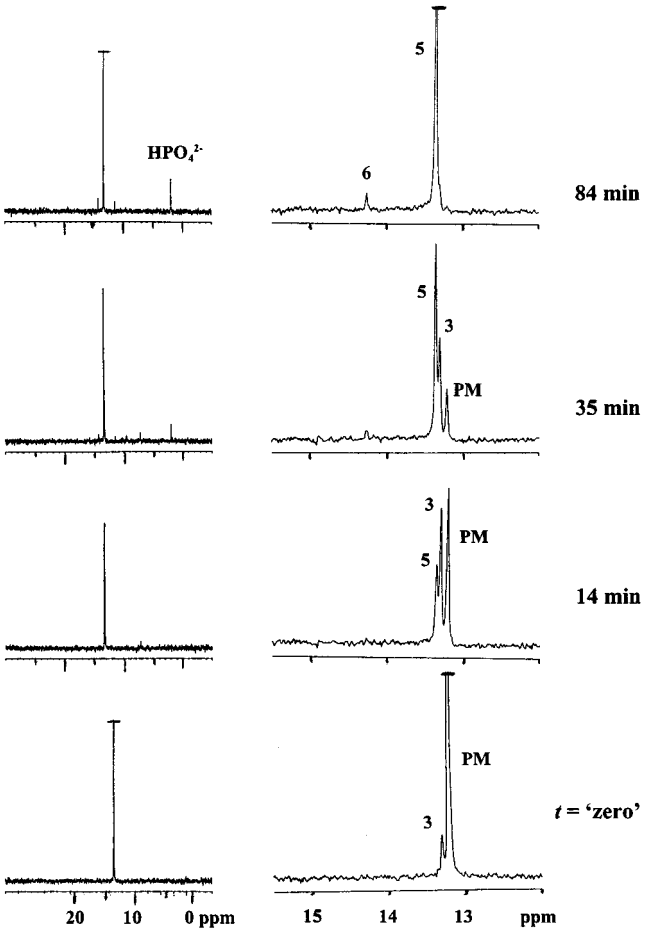

Figure 2. ^{31}P NMR (202.5 MHz) time-averaged spectra recorded as a function of time for the reactions of 11 mM PM with 110 mM GSH in bis-Tris (0.22 M, pH 7.4) at 37 °C. The designated times refer to the start of spectral acquisition with time zero being several minutes after placement of the sample in the NMR probe (and 10−15 min after sample preparation). Left-hand column: full display. Right-hand column: partial display, expanded to show individual signals. Chemical shifts (δ): PM, 13.20; **3**, 13.29; **5**, 13.33; **6**, 14.24; inorganic phosphate (P_i), 1.9. Signals shown "cropped" at times zero and 84 min were off-scale on these displays.

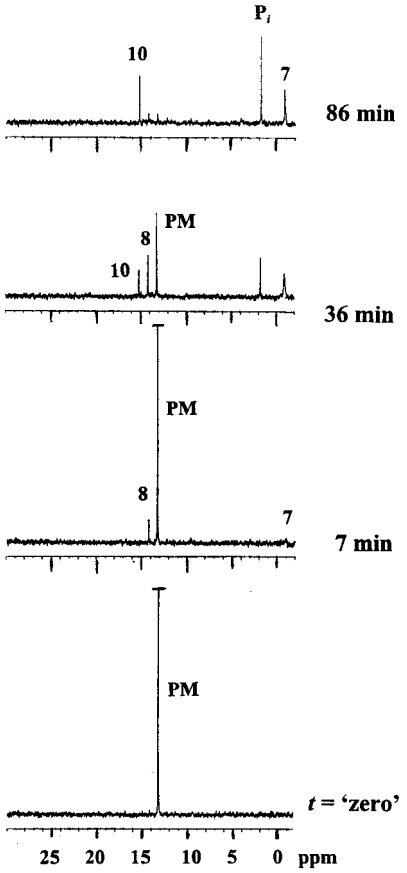

Figure 3. ^{31}P NMR (202.5 MHz) time-averaged spectra recorded as a function of time for the reactions of 11 mM PM in bis-Tris (0.22 M, pH 7.4) at 37 °C. The designated times refer to the start of spectral acquisition with time zero being several minutes after placement of the sample in the NMR probe (and 10−15 min after sample preparation). Chemical shifts (δ): PM, 13.20; **8**, 14.16; **10**, 15.17; **7**, −1.0; inorganic phosphate (P_i), 1.9. Signals for PM at times zero and 7 min were off-scale on these displays.

and (c) similar work in the literature by us and others.[7,9,10,13,20,22] Because of the sensitivity of ^{31}P NMR chemical shifts to pH, temperature, concentration, and solvent, some values given herein may not match previously reported work.

With 110 mM GSH, the resonance for PM (δ 13.20) decreased with the concomitant growth of a major, but transient, resonance at δ 13.29. The disappearance of this intermediate was linked to the formation of a reasonably stable product at δ 13.33 (Figure 2). This sequence, well documented for thionylations of PM, represented the conversion of PM to monoglutathionylated **3** and, ultimately, bisglutathionylated **5**.[7,9,13,22] By way of comparison, the ^{31}P shifts for PM, **3**, and **5** have been reported as approximately 13.68, 13.73, and 13.71, respectively (0.07 M phosphate, pH 7.0, 24 °C, initial concentrations of 6 mM PM and 60 mM GSH).[7] While the shifts were not identical in the two experiments, neither were the conditions; however, the signal intensities and patterns of growth and disappearance left no doubt as to the identifications of these resonances.

An additional signal at δ 14.24 appeared during the course of the reaction and the persistence of this resonance indicated that it represented a stable end product ($\tau_{1/2}$ much greater than that of any precursor). Even after 2 h of reaction time, however, this signal accounted for only 4% of the total phosphorus intensity while that for bisglutathionylated **5** was 72% (Figure 2). The signal did not appear in spectra of solutions without GSH. These data were consistent with assignment of the resonance to monoglutathionylated, monohydroxylated **6**, the product formed from two sequential alkylation reactions involving different nucleophiles (i.e., GSH and water).

In the absence of any GSH, one NMR experiment was initiated quickly enough such that the only signal observed in the "time zero" ^{31}P spectrum was that for PM (Figure 3). Two additional signals appeared simultaneously in the spectrum taken at $t = 7$ min. These resonances were attributed to monohydroxylated intermediate **8** (δ 14.16) and P−N bond hydrolysis product **7** (δ −1.0), as supported through considerations of kinetic characteristics, literature reports,[7,9,10,13] and/or use of authentic material (**7**).[20] In subsequent spectra, signals appeared which were consistent with bishydroxylated **10** (δ 15.17) and inorganic phosphate (δ 1.9).

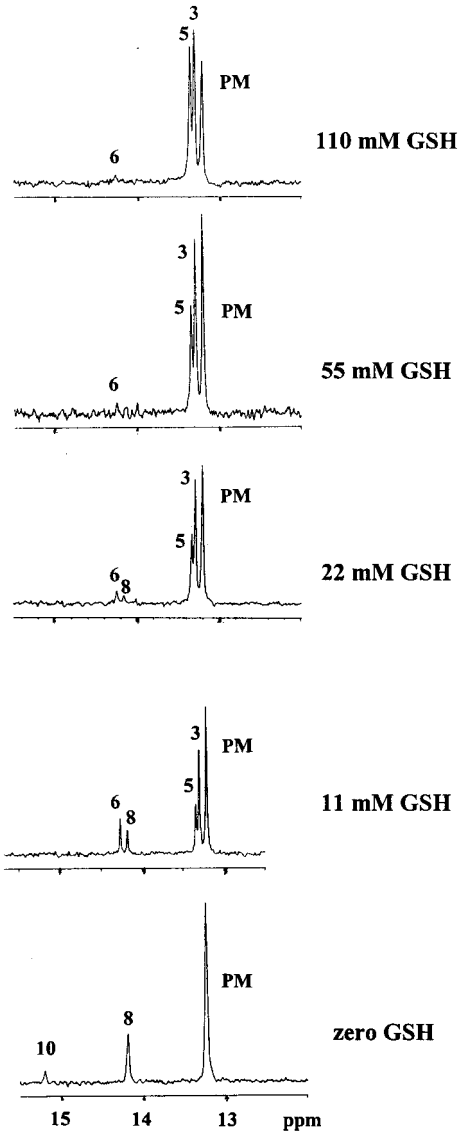

Figure 4. ^{31}P NMR (202.5 MHz) time-averaged spectra recorded for the reactions of 11 mM PM with varying initial concentrations of GSH in bis-Tris (0.22 M, pH 7.4) at 37 °C. Each spectrum shown was recorded at t = ca. 21−22 min (slightly greater than one half-life for PM).

Spectra obtained from solutions of PM with 11 mM GSH contained features of those obtained with zero and 110 mM GSH. Increasing concentrations of GSH (22 and 55 mM) provided spectra which were more similar to those obtained with 110 mM GSH. This trend resulted from a decreased influence of water as a nucleophile and an increase in the product distribution derived from reactions wherein GSH was the nucleophile (Figure 4).

The stability of each alkylation end product (**5**, **6**, **10**) was assessed by comparing changes in peak intensities between times when all precursors (**1**, **3**, **8**) were no longer visible (t = 2 h) and t = 17−21 h. The average variations in peak heights were as follows: for bisglutathionylated **5**, ±9% (n = 5); for monoglutathionylated, monohydroxylated **6**, ±10% (n = 5); and for bishydroxylated **10**, +9% (n = 4). Compounds **5**, **6**, and **10** were thus defined as end products based on the fact that the half-life of each was much greater than the half-life of any precursor. Over time, however, there was a slow loss of the alkylated end products and this was apparently linked to the formation of minor resonances around δ 4. Tentatively, these resonances were attributed to products of the type $(NuCH_2CH_2)_2N-PO_3H^-$ based on similarities in chemical shift to that of synthetic $(ClCH_2CH_2)_2N-PO_3H^-$ (δ 4.6).

Table 1. Fractional Distribution of Alkylation Products for Reactions of 11 mM PM in 0.22 M Bis-Tris at pH 7.4, 37 °C (from ^{31}P NMR Data)

mM GSH (initial concn)[a]	compd **5**	compd **6**	compd **10**
0	na[b]	na	0.13 (0.12−0.14)[c]
11	0.21 (0.19−0.22)	0.22 (0.21−0.23)	0.03 (0.03−0.04)
22	0.50 (0.47−0.52)	0.14 (0.13−0.15)	nd[d]
55	0.70 (0.64−0.76)	0.08 (0.07−0.09)	nd
110	0.72 (0.71−0.72)	0.04 (0.04−0.05)	nd

[a] GSH concentrations decreased over time as GSH was consumed in the alkylation reactions. [b] Not applicable. [c] Average value and, in parentheses, the range of values (n = 2). [d] Not detected.

Using the final spectrum of each experiment ($t \geq 8$ h), each alkylation end product was quantified by measuring its signal intensity relative to the total phosphorus intensity in the spectrum (i.e., the total intensity of all signals, assigned or not). These results are shown in Table 1 with the PM alkylation end products expressed as fractional distributions. In each case, the remainder of the fraction is attributed primarily to P−N bond hydrolysis products as well as to low levels of undetected HOH alkylation products. It should also be pointed out that the cyclohexylammonium salt of PM was used in these experiments. Under the conditions of these experiments (pH 7.4), cyclohexylamine (pK_a 10.64)[23] was not expected to participate as a nucleophile in the reaction manifold in any significant manner.

The data in Table 1 indicate that in the presence of a weak nucleophile (55 M H_2O, no GSH) only 13% of the PM underwent bisalkylation. Exposure to a strong nucleophile (GSH) increased the occurrence of bisalkylation but in all cases, P−N bond hydrolysis was a significant factor.

Kinetic Analysis of NMR Data for PM Reactivity. The results presented in Table 1 were derived from a single spectrum taken at the end of each kinetic run. It was desirable to consider a more rigorous treatment of the data. Thus, a kinetic model was constructed consisting of the system of rate equations that mathematically describes the precursor−product pathways shown in Scheme 2. The analysis utilized ^{31}P NMR peak height data from an average of 15 spectra per kinetic run.

Nonlinear regression analysis was used to fit the kinetic model for the data from each of the replicate experiments (n = 2) at the following concentrations of GSH: zero, 11, 22, 55, and 110 mM. These fits yielded rate constants and product distributions. The consistently excellent fit of the data by the kinetic model is demonstrated in Figure 5. Kinetic modeling of both HOH alkylation and P−N bond hydrolysis reactions was only possible for data arising from experiments with zero or low concentrations of GSH (11 and 22 mM). At high GSH concentrations (55 and 110 mM), the preponderance of GSH alkylation resulted in concentrations of HOH alkylation products that were too small (<10%) to be monitored reliably using NMR.

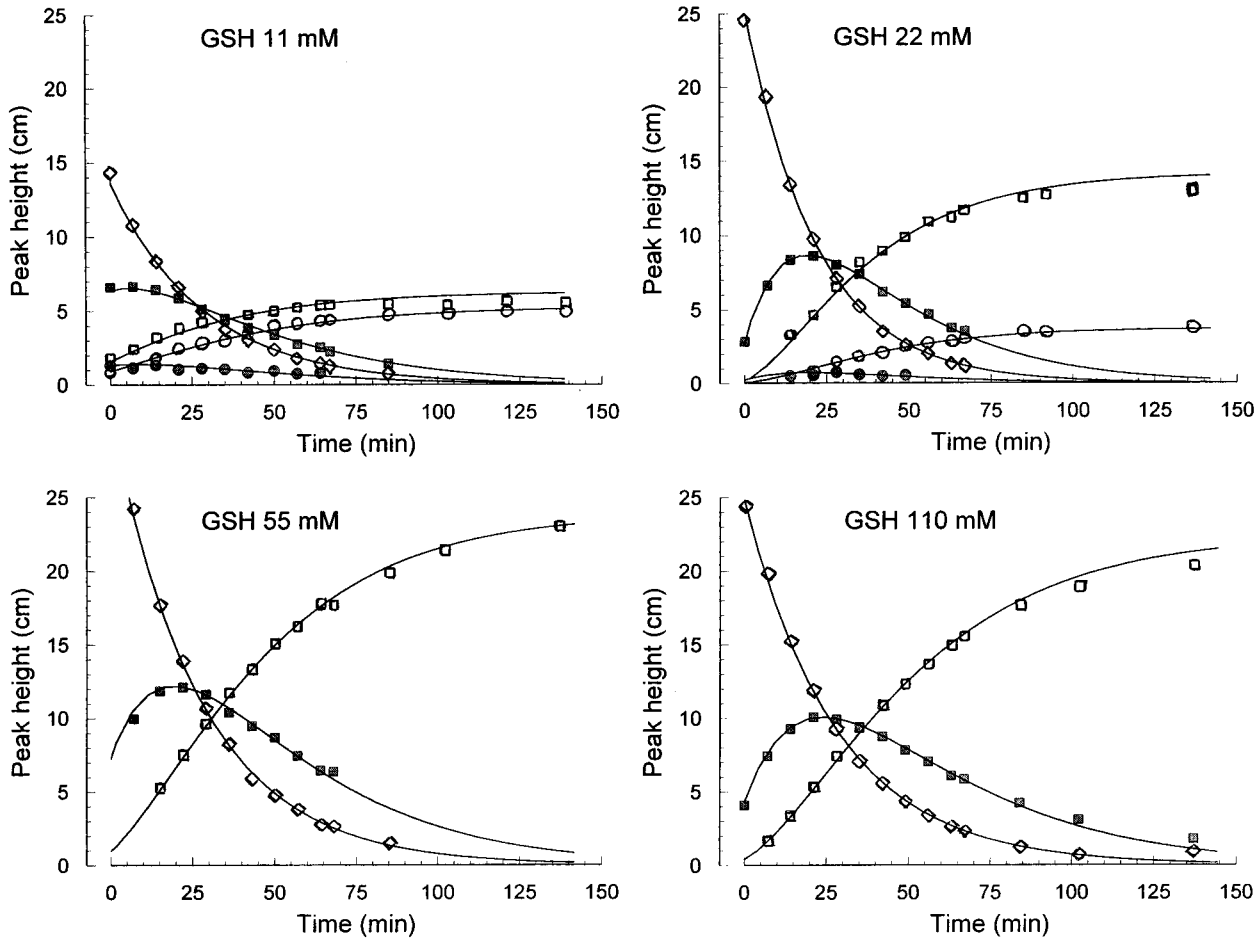

Figure 5. Representative time courses of the ^{31}P NMR peak heights of PM (11 mM) and its alkylation products in the presence of various concentrations of GSH (pH 7.4, 37 °C). The symbols are the observed data (average of two runs), and the solid lines are the computer fits of the data. Open diamonds, PM; filled circles, monohydroxylated **8**; open circles, monohydroxylated, monoglutathionylated **6**; filled squares, monoglutathionylated **3**; and open squares, bisglutathionylated **5**.

Table 2. Fractional Distribution of the Alkylation End Products Predicted for Reactions of 11 mM PM in 0.22 M Bis-Tris at pH 7.4, 37 °C

mM GSH (initial concn)[a]	compd **5**	compd **6**	compd **10**
0	na[b]	na	0.10
11	0.22	0.19	0.04
22	0.45	0.11	<0.01
55	0.55	nm[c]	nm
110	0.75	nm	nm

[a] Modeling was done assuming that the GSH concentration decreased over time as GSH was consumed in the alkylation reactions. [b] Not applicable. [c] Not modeled.

Table 2 shows the values for the distribution of alkylation end products as predicted by kinetic modeling. Using the mean kinetic parameter values as estimated from the experimental data, the time courses of HOH alkylation, GSH alkylation, and P−N bond hydrolysis were computer simulated at each of the GSH concentrations studied. The simulations were carried out to 6 h to ensure that the simulated reactions had progressed to completion. The distribution estimates reflect the fact that, except at the highest GSH concentration, there was appreciable reduction in the GSH concentration in the reaction mixtures over time as a result of consumption of GSH in the alkylation reactions. In the presence of only a weak nucleophile, i.e., water (55 M), it was predicted that just 10% of the PM completed the bisalkylation pathway giving bishydroxylated **10**. The remainder of the PM ultimately gave rise to products of P−N bond hydrolysis. Increasing concentrations of a stronger nucleophile, i.e., GSH, resulted in a decrease in the generation of P−N bond hydrolysis products and an increase in the formation of bisalkylation products and, in particular, those products derived from alkylation of the stronger nucleophile (i.e., **6** and, especially, **5**). As shown in Figure 5 and through a comparison of Tables 1 and 2, the end product distributions given by a direct analysis of the NMR data agreed very well with that which was predicted by the kinetic modeling. This agreement validated the selection of spectra at $t \geq 8$ h as displays of final product arrays.

Through monoalkylation, the nucleophile becomes a substituent and, as such, must have an effect on the rate of the second alkylation reaction. Quantification of this influence on PM reactivity is important to an understanding of how monoconjugation may affect subsequent cross-linking and inactivation reactions. In this study, the relative effects of Cl, SG, and OH on the second alkylation reaction were determined by calculating the rate constants for the rate-limiting step in each alkylation reaction, i.e., the formation of each aziridinium ion **2**, **4**, and **9** (Table 3). The rate of formation of **2** was consistent with previously published data under comparable conditions of pH and temperature

Table 3. Mean Value of the Rate Constant for Aziridinium Ion Formation (pH 7.4, 37 °C)

reaction	k (min^{-1})	range of values for k (min^{-1})	n[a]
PM → **2**	0.0406	0.0311−0.0556	10
3 → **4**	0.0359	0.0276−0.0497	8
8 → **9**	0.0486	0.0455−0.0563	6

[a] Number of values.

Table 4. Predicted Fractional Distribution of Aziridinium Ions[a] among Alkylation and Hydrolysis Reactions at pH 7.4, 37 °C, Given Constancy of the GSH Concentration

mM GSH[b]	HOH alkylation	GSH alkylation	P−N bond hydrolysis
0	0.31	na[c]	0.69
11	0.11	0.64	0.25
22	0.07	0.78	0.15
55	nm[d]	0.77	nm
110	nm	0.87	nm

[a] The partitioning among alkylation and P−N bond hydrolysis reactions was assumed to be the same for each aziridinium ion **2**, **4**, and **9**. [b] Modeling was done assuming *constancy* of the GSH concentrations. [c] Not applicable. [d] Not modeled.

(i.e., 0.0406 min^{-1} versus 0.0354−0.0486 min^{-1}).[9,10,13] Across experiments, the rate constant for the formation of glutathionylated aziridinium ion **4** was consistently 89% as large as the value of the rate constant for the formation of aziridinium ion **2**. Conversely, the rate constant for the formation of hydroxylated aziridinium ion **9** was, on average, 124% that for formation of aziridinium ion **2**. Thus, relative to Cl as a substituent, SG was found to retard aziridinium ion formation while OH accelerated it. Although this is a trend opposite to what would have been predicted based on electronegativities and their impact on the nucleophilicity of the reacting nitrogen, the same rate retardation effect has been reported for analogous reactions of GSH and nitrogen mustards.[24] The rates of aziridinium ion formation from monoglutathionylated chlorambucil and melphalan are 90−91% that of their chlorinated counterparts (pH 7.4, 37 °C, 1.5% DMSO). The literature does not provide the same agreement with respect to the substituent effect of OH on aziridinium ion formation. For the formation of hydroxylated aziridinium ion **9**, Watson et al. reported rate constants (0.0310−0.0500 min^{-1})[10] which were similar to ours but which did not establish a pattern for the effect of OH relative to Cl.

Table 4 shows the distribution of aziridinium ion reaction products as a function of GSH concentration based on the mean values of the partition constants as estimated from the experimental data *and given constancy of the GSH concentrations* (as would obtain were the PM concentration low relative to the initial GSH concentration, e.g., in vivo). These reaction distributions apply to each of the three aziridinium ions (**2**, **4**, and **9**) because the partitioning between alkylation and P−N bond hydrolysis was assumed to be the same for each. With this assumption, then, the partitioning estimates can be used to calculate the distributions of all intermediates as well as end products. With respect to end product distributions, the results given by Table 4 are virtually the same as those given in Table 2 under conditions where GSH consumption is negligible (i.e., [GSH] ≫ [PM]; 55 and 110 mM GSH). When [GSH] ≈ [PM], there is more variance between Tables 4 and 2. This is a reflection of the fact that the data in Table 4 is based on a constant GSH concentration while that in Table 2 is not.

On the basis of the reaction partitioning given in Table 4, then, the general predictions and implications for reactions of PM (11 mM) at pH 7.4 are as follows. *In the presence of a high, unchanging concentration of a weak nucleophile (55 M H_2O),* PM forms aziridinium ion **2**, and 31% of this ion alkylates water to give a monohydroxylated intermediate; 69% of the ion undergoes P−N bond hydrolysis. The monohydroxylated intermediate forms a second aziridinium ion which undergoes the same partitioning (31% alkylates water, 69% undergoes P−N bond scission). *The net result is that only 10% of the original PM is predicted to successfully undergo bisalkylation of the weak nucleophile (water).*

In the presence of a high, unchanging concentration of a strong nucleophile (110 mM GSH), the data in Table 4 predicts that PM forms aziridinium ion **2** and then 87% of this ion alkylates GSH to give a monoalkylated intermediate. The remainder of **2** (13%) partitions between P−N bond hydrolysis and HOH alkylation. Recalling that the relative rates of reaction are 0.69 (P−N bond hydrolysis) and 0.31 (HOH alkylation), the predicted partitioning is 9% P−N bond hydrolysis (0.69 × 13%) and 4% HOH alkylation (0.31 × 13%). Of the monoglutathionylated intermediate, 87% goes on to react with more GSH while the remainder undergoes P−N bond hydrolysis (9%) and HOH alkylation (4%). *The net result is that 76% of the original PM is predicted to undergo bisalkylation with GSH; 24% of the PM goes on to provide for products of P−N bond hydrolysis (17%) and HOH alkylation (7%).* Concentrations of GSH between these two extremes give intermediate values of alkylation and P−N bond hydrolysis. Extrapolations of the data show that increasing the concentration of GSH will further decrease the significance of the hydrolysis pathway relative to alkylation.

While this study used a very strong (GSH) and a very weak (H_2O) nucleophile, there is literature to support the generality of the data and its implications. Lu and Chan have reported a 32% conversion to CEZ for 0.14 mM PM in 67 mM phosphate at pH 7.4.[12] At that low concentration of PM, the concentration of phosphate would, for all practical purposes, be constant. We can, therefore, compare the results for phosphate (a nucleophile of moderate strength) with those given by Table 4 for GSH under similar conditions (55 mM). Our data indicates that with the stronger nucleophile less PM is converted to CEZ [77% of **2** alkylates GSH and the remainder (23%) partitions between P−N bond hydrolysis (69%) and HOH-alkylation (31%); 69% of 0.23 = 16% CEZ formation]. These results are consistent with our conclusion that product distribution is linked to nucleophile strength; i.e., the stronger the nucleophile, the greater the yield of alkylation end products and, necessarily, the lower the yield of P−N bond hydrolysis products (e.g., CEZ).

Kinetic Analysis of HPLC Data for PM Reactivity. Kinetic modeling was also performed on data derived from HPLC analyses of PM reactivity (see the Experimental Section for details). With HPLC, lower reactant concentrations could be achieved than was

convenient in the ^{31}P NMR experiments. Compatability of the HPLC and NMR results were, therefore, a measure of the relevance of the kinetic conclusions to varied conditions and analytical techniques.

The data from three experiments were analyzed (in each experiment, $n = 1$): PM (1 mM) alone, PM (1 mM) and GSH (10 mM), and PM (1 mM) and thiosulfate (50 mM). All experiments utilized tritiated PM (for peak detection in chromatograms) and were carried out in 25 mM triethanolamine buffer at pH 7.2, 37 °C. Peak assignments were based on considerations of kinetics, UV absorption (for glutathionylated species), and literature reports of the same or similar compounds.[10,25]

For the experiment with PM alone, the time courses of the changes in concentrations of PM, monohydroxylated **8**, and bishydroxylated **10** were modeled. The rate constants for the formation of aziridinium ions **2** and **9** were 0.0397 and 0.0439 min^{-1}, respectively. The fraction of each azirididinium ion undergoing HOH alkylation was 0.33; this allowed for the prediction that 11% (0.33×0.33) of the end products would be bishydroxylated **10**.

For the experiment with 10 mM GSH, the time courses of the changes in concentrations of PM, monoglutathionylated **3**, and bisglutathionylated **5** were modeled assuming constancy of the GSH concentration. The rate constant for the formation of aziridinium ion **2** was 0.0311 min^{-1} and that for the formation of aziridinium ion **4** was 0.0318 min^{-1}. The fraction of each aziridinium ion experiencing GSH alkylation was 0.52; it was predicted, therefore, that 27% (0.52×0.52) of the end products would be bisglutathionylated **5**.

For the experiment with 50 mM thiosulfate, the time courses of the changes in concentrations of PM, the thiosulfate monoalkylated intermediate, and the thiosulfate bisalkylated end product were modeled using a kinetic model identical with that used for GSH alkylation. The rate constant for the formation of aziridinium ion **2** was 0.0323 min^{-1} while that for the formation of the second aziridinium ion was 0.0291 min^{-1}. The fraction of each aziridinium ion reacting with thiosulfate was 0.85; thus, the product of bisalkylation with thiosulfate would account for 72% (0.85×0.85) of the final product array.

The HPLC-derived kinetic parameters compared very favorably with those given by the NMR data. The rate constants for formation of aziridinium ions **2** and **4** fell within the ranges of those found by NMR and that for **9** was quite close (Table 3).

The results from the HPLC and NMR methods confirmed that the distribution of alkylation products was directly dependent on the relative concentrations of the nucleophiles in the reaction mixture. Variations in PM concentrations had no bearing on the product distribution. Because the HPLC-derived results given above were determined assuming that the nucleophile concentration was constant throughout the reaction period, comparisons were made with the NMR-derived results calculated with the same assumption, i.e., those given in Table 4. Thus, with water as the only nucleophile, 11% of PM was predicted by HPLC to undergo bisalkylation as compared with 10% by NMR. In the presence of 10−11 mM GSH, 27% of the product was predicted by HPLC to be bisglutathionylated versus 41% by NMR. Thiosulfate and GSH are both relatively strong nucleophiles, and therefore, it was expected that similar concentrations would lead to similar product distributions. Such was found to be the case: 50 mM thiosulfate led to 72% bisalkylation product (HPLC) while 55 mM GSH gave 76% bisglutathionylated product (NMR).

As noted previously, for reactions of GSH with either chlorambucil or melphalan, the rate of formation of the second aziridinium ion has been reported to be about 10% slower than that of the first.[24] A similar rate decrease was given by our NMR data for reactions of PM with GSH. For reactions of thiosulfate with either chlorambucil or melphalan, it has been reported that the rate constant for the formation of the second aziridinium ion decreases by more than 40% relative to that of the first.[24] Such a significant substituent effect was not found for the thiosulfate adduct of PM (rate for the first aziridinium ion, 0.0323 min^{-1} and for the second, 0.0291 min^{-1}); however, this result was based on a single experiment.

Interactions between Buffer and PM. There is much data in the literature to support the conclusion that the *half-life* of PM is independent of buffer type.[9,10,13] On the other hand, during the course of the NMR studies it was found that PM can give a *product array* which is very buffer-dependent. In every buffer studied (bis-Tris, lutidine, triethanolamine, and Tris), ^{31}P NMR signals were observed which could not be attributed to products of GSH or HOH alkylation or P−N bond hydrolysis. The intensities of these unassigned signals decreased with increasing concentrations of GSH and/or decreasing concentrations of buffer. The buffer−PM interactions which gave rise to these signals were not obvious because each buffer studied was considered to be nonnucleophilic.

Figure 6 shows spectra of 11 mM PM in 110 mM buffer after 1 h of reaction at 37 °C. Extraneous signals were observed in each of the buffers studied; however, bis-Tris was the buffer which was least interactive with PM at the concentrations used for the NMR analyses. For 11 mM solutions of PM, a minimum of 20 molar equiv of bis-Tris was required to maintain the pH at 7.4 over the course of the study (8−21 h). At this concentration, signals from side reactions remained minimal and spectral interpretations of the PM reactions of interest were easier. Thus, 220 mM bis-Tris was selected as the buffer solution for the ^{31}P NMR studies of the chemistry of PM. While the HPLC studies utilized triethanolamine as the buffer, the concentrations were so low (1 mM PM in 0.25 mM buffer) that any buffer−PM interactions were expected to be insignificant.

Conclusion

The cumulative experimental and theoretical data cited above support the hypothesis that, at neutral pH, P−N bond hydrolysis occurs in aziridinium ion **2** to give CEZ (path C, Scheme 1). That CEZ is formed from **2** rather than from NNM is supported in a compelling manner by the observed dependence of P−N bond scission on GSH concentration (the direct hydrolysis of PM to NNM would not be influenced by the presence of added nucleophiles). While the given arguments may

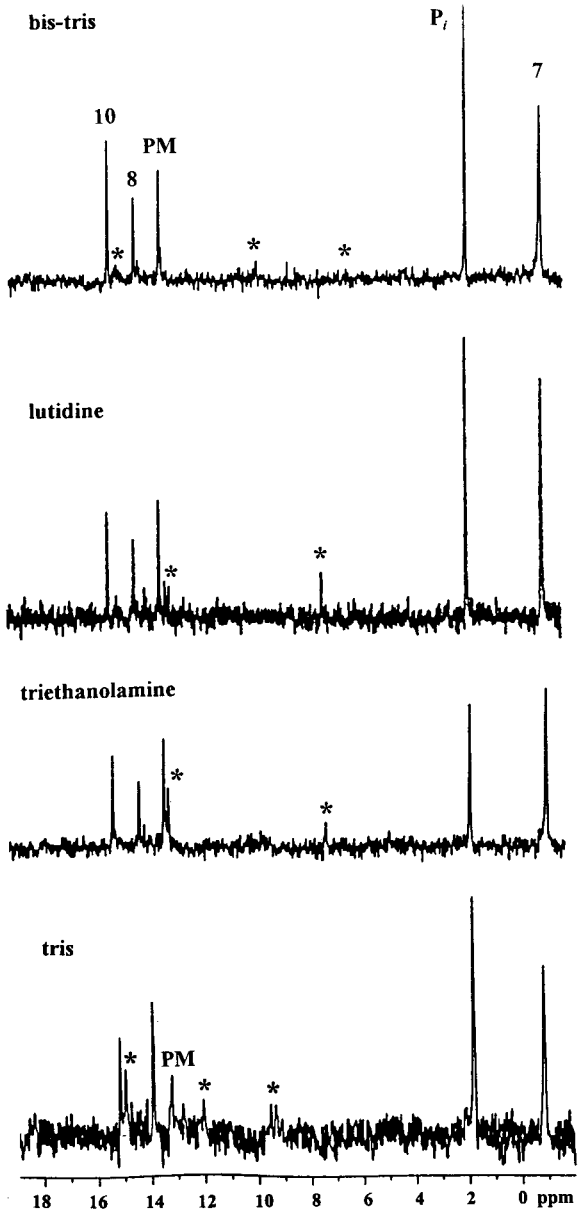

Figure 6. ^{31}P NMR (202.5 MHz) time-averaged spectra recorded for the reactions of 11 mM PM in varying buffers (110 mM) at pH 7.4, 37 °C. Each spectrum was recorded at $t \approx 1$ h. Starred resonances appeared to arise from interactions between buffer and PM (or components derived from PM). The intensities of these resonances were dependent on the concentrations of buffer and PM.

not exclude a contribution from NNM in the formation of CEZ, they suggest that P−N bond hydrolysis in **2** is the most significant if not exclusive mechanism by which CEZ is formed at neutral pH. This pathway can occur under both in vitro and in vivo conditions and there is precedent for each: it has been reported that NNM cannot be detected in neutral, buffered solutions of PM[12] or in the plasma of CP-treated patients and rats.[26,27]

It is noteworthy that hydrolytic P−N bond scission in **2** would be a pH-independent process. This is in contrast to any P−N bond hydrolysis which might occur in PM itself, prior to aziridinium ion formation. We have shown previously that the pK_a of 4.9 which is associated with PM refers to protonation of the NH_2 moiety.[20] Thus, even though path B (Scheme 1) may not contribute to the chemistry of PM at neutral pH, it remains the likely mechanism by which PM hydrolyzes under acidic conditions.

In view of these findings regarding the production, or lack thereof, of NNM from PM at neutral pH, numerous literature reports must be reconsidered. References to the "well-known formation of NNM from PM" are often based on earlier works which actually are speculative in nature. This problem is compounded when the conditions of pH are not included. In a given analysis, other sources of NNM must also be considered. For example, it has been shown that the CP metabolite carboxyphosphamide hydrolyzes to NNM under acidic conditions; coupled with sample handling, this could account, at least in part, for the NNM found by some (but not others) in patient urine and plasma.[10,12,28,29] Another consideration is that some methods of analysis involve trapping agents which will not discriminate between NNM and CEZ. Given that NNM rapidly forms CEZ at pH 7.4 (e.g., $\tau_{1/2} = 17$ min at 37 °C), exactly what species is being used as a standard for 'authentic compound' must also be clarified. The lifetime of NNM will, of course, be pH dependent (pK_a 7.40, see the Experimental Section).

Reactions between GSH and PM are spontaneous and irreversible and, therefore, represent a mode of detoxification. The previously reported inability to detect (by mass spectrometry) any GSH−PM alkylation products formed spontaneously at pH 7 is puzzling.[6] Perhaps under the conditions of the experiment, which were not given, the concentrations of such products were too low to be detected. In any case, the more significant finding reported herein is that, for the first time, nucleophile strength and concentration were found to impact on the distribution of alkylation and hydrolysis products given by PM. In short, the stronger and more concentrated the nucleophile, the greater the yield of alkylation end products and, necessarily, the lower the yield of P−N bond hydrolysis products (e.g., CEZ).

The implications of the kinetic data to the in vivo situation are many. Given the multitude of endogenous nucleophiles available, one can imagine the impact on the distribution of possible products in an expanded Scheme 2. Cellular phosphate, alone, is expected to participate in a significant way, as has been shown for the alkylation reactions of melphalan.[25] Among all the nucleophiles in vivo, it is hard to predict the relative nucleophilicity of the N-7 position of a guanine residue in an intact DNA helix; however, it is interesting to point out that alkylation and P−N bond hydrolysis are not mutually exclusive pathways when considering the mechanism of DNA cross-linking. Alkylation of a guanine residue by aziridinium ion **2** could provide the initial link; subsequent formation of the second aziridinium ion could lead to loss of the phosphoramidate group. The actual cross-link would be completed through a CEZ-like intermediate with second-order kinetics.

The nature of the PM−buffer interactions which were detected remains unclear. At the least, this observation serves as another warning that the chemistry of PM is complex and very condition-dependent.

Given the reactivity of PM, it is almost a wonder that any of this species survives to cross-link DNA. This is not meant to suggest that PM is not the ultimate

alkylator derived from CP but rather that other contributors must also be considered. Much data suggest that PM which is generated extracellularly will not lead to the same level of therapeutic benefits as those achieved by PM which is generated intracellularly.[3,10,30] This is generally attributed to poor membrane permeability of the anionic PM, a factor which would not appear to be an issue with CEZ. At least from transport considerations, the production of neutral CEZ from PM either intra- or extracellularly would seem to be equally beneficial. Since direct administration of PM (or NNM) does not give a particularly good therapeutic index,[3] a major role for CEZ in DNA alkylation might be viewed with some skepticism. The fact that CEZ was found to have "potent activity" in a cytotoxicity evaluation does not alleviate this skepticism; NNM also had "potent activity" in the same screen.[31] Nevertheless, because the importance of circulating PM remains a matter of discussion[10] and because a significant portion of aziridinium ion **2** partitions to hydrolysis, the relevance, if any, of CEZ in the therapeutic efficacy of CP treatment must be addressed. If the chemistry and biologics of CEZ are such that this compound is determined to be an undesirable metabolite, ways to decrease its production from PM can then be considered. Quantum chemical calculations predicting the impact of structural modifications on PM reactivity would be useful in this regard, given the somewhat unexpected trend observed for substituent effects on the rates of aziridinium ion formation (Table 3).

We have begun investigations of some of the questions raised by this work, e.g., the solution chemistry of CEZ, the nature of the DNA cross-linking mechanism, and the distribution of alkylation and P−N bond hydrolysis products in PM analogues such as isophosphoramide mustard.

Experimental Section

Phosphoramide mustard (as the cyclohexylammonium salt) was a gift from the Drug Synthesis and Chemistry Branch, Division of Cancer Treatment, National Cancer Institute. Glutathione was purchased from Sigma Chemical Co. Nornitrogen mustard as the hydrochloride salt [bis(2-chloroethyl)-amine hydrochloride] was purchased from Aldrich Chemical Co. The synthesis of phosphoramidic diacid (in situ from phosphoric triamide) has been reported.[20]

Unless specified otherwise, all NMR spectra were acquired at 11.75 T on a Bruker MSL500 NMR spectrometer. ^{31}P NMR spectra were acquired at 202.5 MHz, and chemical shifts were referenced to external 1% H_3PO_4 in D_2O. ^{1}H NMR spectra at 500.13 MHz were acquired with a sweep width of 5000 Hz, a 60° pulse, 16K data points, and a repetition time of 2.05 s. The free induction decay was multiplied by an exponential apodization factor to yield a line broadening of 0.2 Hz in the frequency spectrum. Chemical shifts were referenced to TSP-d_4.

HPLC instrumentation included a Beckman Instruments System Gold, model 110 pumps, model 406 analogue interface, and model 166 UV detector.

Ab Initio Calculations. Restricted Hartree−Fock (HF)[14−16] self-consistent field (SCF) geometry optimizations were made using a 6-31G* basis set[16] with a gradient convergence criteria at <0.001 Hartree/Bohr (<0.627 kcal) for the change in molecular energy as a function of the atomic displacements between consecutive cycles. All internal degrees of freedom for the structures were optimized without constraints or parametrization. The HF-optimized structures were used for the equilibrium geometries. All ab initio mechanical calculations were made with QUEST.

Kinetic Analysis. A kinetic analysis of the data was undertaken using a kinetic model consisting of the system of rate equations that mathematically describes the precursor−product pathways shown in Scheme 2. The rate constants of formation of the aziridinium ions and the partition constants defining the fractional distribution of precursor among its products were estimated using the model. The formation of aziridinium ions was assumed to follow first order kinetics and to be essentially irreversible under the conditions of the experiments (dilute solutions free from added chloride ions). The formation of aziridinium ions was also assumed to be spontaneous and rate limiting, as supported by previous studies of PM and related compounds.[9,10,13,22,24,25,32] These aziridinium ion intermediates were too short-lived to be observed on the NMR time scale, so the rate of appearance of the mono- and dialkylated species were treated as being equal to the disappearance of their relevant precursors. The partitioning between alkylation and P−N bond hydrolysis products was assumed to be the same for each of the three aziridinium ion intermediates (**2**, **4**, **9**). GSH alkylation reactions were treated as second-order substitution reactions dependent upon the concentration of GSH (which decreased over time as a result of the incorporation of GSH into GSH alkylation products); therefore, the partition constant for GSH alkylation products was modeled as depending upon the concentration of GSH. HOH Alkylation reactions and P−N bond hydrolysis reactions were treated as pseudo first-order so the partition constants for HOH alkylation and P−N bond hydrolysis products were modeled as true constants. It was assumed that no interconversion among products occurred and that alkylation reactions were irreversible over the time frame of the simulation, which was 6 h (for the aziridinium ion formation rate constants used, a period of 5−6 h was required for the reactions to be at least 99% complete). These last assumptions were validated by the long-term stability found in this study for each of the hydroxylated and glutathionylated end products (**5**, **6**, **10**). Nonlinear regression analysis utilized PCNONLIN (Scientific Consulting Inc, Apex, NC).

Chloroethylaziridine (CEZ). (A) Synthesis in Situ. Nornitrogen mustard hydrochloride [bis(2-chloroethyl)amine hydrochloride, 1.8 mg, 0.01 mmol] was dissolved in D_2O (1 mL), and the pD was adjusted to 7−8 using small amounts of 0.1 M NaOD. After ca. 40 min at 37 °C, an aliquot (0.1 mL) of this solution was added to 0.6 mL of phosphate buffer (0.1 M in D_2O, pD 7). An examination of the relative integrations by ^{1}H NMR revealed that >90% conversion to CEZ had occurred: ^{1}H NMR (ca. 20 °C; 500 MHz) δ 3.77 (t, J = 7 Hz, 2H, CH_2Cl), 2.73 (t, J = 7 Hz, 2H, CH_2N), and 1.95 and 1.60 (m, 4H, aziridinyl). [For residual nornitrogen mustard: δ 3.81 (t, J = 7 Hz, CH_2Cl) and 3.32 (t, J = 7 Hz, CH_2N).]

(B) Reactivity with Glutathione (GSH). An aliquot (0.1 mL) of ca. 10 mM CEZ (made in situ as described above) was added to 1.0 mL of a solution of 10 mM GSH in 0.1 M phosphate (made with 100% D_2O) at pD 6.9. The solution pD was adjusted to 7 with 0.1 M NaOD, and the disappearance of CEZ (ca. 1 mM) was then monitored by ^{1}H NMR (500 MHz) at 37 °C. Spectra were acquired every 3.4 min over a time period of 2 h (during which time the pD dropped to 6.8), and shifts were referenced to the HOD resonance at δ 4.65. The data (changes in signal integration) was analyzed using a nonlinear least-squares fit assuming a pseudo-first-order process for the disappearance of CEZ. This gave an estimated rate constant of 0.0130 min^{-1} ($\tau_{1/2}$ = 53 min) for the reaction of CEZ (ca. 1 mM) with GSH (ca. 10 mM).

(C) pK_a Determination. An NMR sample of 1 mM nornitrogen mustard hydrochloride in 5% D_2O was heated at 37 °C for ∼20 min so as to effect partial conversion to CEZ. In sequence, the sample was cooled in an ice/water bath, the pH was read, a proton NMR spectrum (200 scans) was acquired at 5 °C, and the sample pH was checked again at low temperature. The pH readings had to agree within 0.1 pH units for the data to be used for the pK_a determination. The pH of the sample was then adjusted to a new value with 0.1 M NaOH or 0.1 M HCl, and the sequence was begun again.

In this manner, a total of 13 spectra were collected over a pH range of 1.8 to 10.4. The pH values were not corrected for deuterium isotope effects, sample temperature, or calibration of the pH meter at 20 °C. The chemical shifts of select resonances for CEZ and NNM were plotted versus pH (a capillary insert containing TSP in D_2O served as the chemical shift reference). A single sigmoidal curve was fit to each data set giving a pK_a value of 6.62 for CEZ and 7.40 for NNM.

^{1}H NMR Experiment with PM. PM [0.026 mmol, 5.8 mg of the free acid (synthesis described below)] was dissolved in D_2O (2.0 mL) at 37 °C. The pD of the solution (∼2.9) was adjusted to 7.5 by the addition of small amounts of 0.1 M NaOD. The pD of the solution was maintained between 7.0 and 7.5 by regular additions of 0.1 M NaOD during the course of the experiment. At specific time intervals, an aliquot (0.05 mL) of the reaction solution was removed and added to 0.6 mL of an ice-cold buffer solution of 0.05 M sodium phosphate in D_2O (containing 0.27 mM TSP-d_4) at pD 7.4. Each sample (1 mM PM) was then immediately frozen and stored in liquid nitrogen until spectral analysis (ca. 30−60 min after freezing). For the spiking experiment, a second 0.05 mL aliquot was taken at $t = 45$ min, and to this was added 0.05 mL of freshly made 13 mM nornitrogen mustard hydrochloride in D_2O. After being diluted with 0.55 mL of the phosphate buffer, the sample (1 mM PM and 1 mM nornitrogen mustard) was frozen as described above. Just prior to spectroscopy, the aliquot of interest was thawed and a ^{1}H NMR spectrum was then obtained at a probe temperature of 5 °C. The results are shown in Figure 1.

Spectra were obtained at 500 MHz on a Varian Unity spectrometer using a 60° proton pulse, a sweep width of 5600 Hz, an acquisition time of 3.1 s, and a relaxation delay of 2.5 s. Free induction decays were collected into 32K data points and processed by multiplying with an exponential filter resulting in a line-broadening of 0.5 Hz in the frequency spectrum.

The pD of each solution was obtained using a combination electrode and was the actual meter reading, uncorrected for deuterium isotope effects.

^{31}P NMR Experiments with PM. NMR samples were prepared immediately prior to use. In a glass vial, phosphoramide mustard (PM) as the cyclohexylammonium salt (8.8 mg, 0.0275 mmol) was dissolved in a combination of D_2O (0.25 mL) and 1 M bis-Tris [0.550 mL, pH 7.4 (adjusted with nitric acid)]. When glutathione (GSH) was utilized, a solution of GSH (1, 2, 5, or 10 molar equiv relative to PM) in H_2O (1.70 mL) was immediately added to the NMR sample containing PM. When no GSH was used, water (1.7 mL) was added instead. The pH of the NMR sample was adjusted to 7.40 (±0.04) using 1 M NaOH and/or 2−3 M HNO_3. The solution was immediately transferred to a 10 mm NMR tube and placed in an ice bath. Within 10 min, the NMR tube was placed in the spectrometer probe (preheated to 37 °C). The sample was allowed to thermally equilibrate for 2−3 min before optimization of the magnetic field homogeneity.

At time "zero", which was approximately 20 min after dissolution of the PM, 202.5 MHz ^{31}P NMR acquisition was initiated using an 8 kHz spectral window, 16K data points, a 45° pulse of 10 μs, gated low-power ^{1}H decoupling, and a pulse recycle time of 6.25 s. The free-induction decay (FID) signal that was obtained after 32 pulses was stored in the computer and the next spectral acquisition was initiated at time t, relative to "zero" time. While each time t refers to the start of a spectral acquisition, each spectrum displays an averaged set of signals obtained over 3.3 min of reaction time (32 pulses). Spectra were accumulated every 3.5 min during the first 2 h of each experiment; a final spectrum was taken at some time period between 8 and 21 h (and in at least one run under each set of conditions, a final spectrum was taken at $t \geq 17$ h). Prior to Fourier transformation, the averaged FID signal was multiplied by an exponential function so as to result in an additional 2 Hz line broadening in the frequency domain spectrum. Upon completion of each NMR experiment (8−21 h), the pH of the sample was checked again; variations of no more than ±0.2 pH units were considered acceptable.

Signal intensities (peak heights) were used to measure the relative concentrations of components as a function of time. For a PM reaction sample containing all of the species shown in Scheme 2, spectra were acquired using varied pulse delay times (5−20 s); within experimental error (±10%), these spectra were all superimposable. This indicated that a 6.25 s pulse delay was sufficient to compensate for the differences in relaxation times among the components of interest. Nevertheless, there are inherent errors (±10%) associated with peak height measurements even when using gated decoupling (to supress possible differential nuclear Overhauser effects) and an appropriate pulse delay. Phosphate presents a particular problem in that it can give a very broadened and poorly detected signal. In experiments with high GSH concentration, there was no appreciable loss of aggregate signal over time, and this was probably due to the fact that relatively little of the phosphorus ended up as phosphate.

***N,N*-Bis(2-chloroethyl)phosphoramidic Diacid Dicyclohexylammonium Salt.** A solution of benzyl alcohol (20 mmol, 2.07 mL) in benzene (20 mL, dried, distilled) was added dropwise to a suspension of washed (3 × 20 mL benzene) NaH (0.96 g of a 60% oil dispersion, 24 mmol) in benzene (20 mL) at 5 °C (ice/water bath) and under N_2. Upon complete addition, the reaction mixture was stirred at room temperature for 2 h. The resultant suspension was then added slowly via syringe to a solution of *N,N*-bis(2-chloroethyl)phosphoramidic dichloride [10 mmol, 2.59 g, $(ClCH_2CH_2)_2NP(O)Cl_2$, available through Aldrich Chemical Co. or can be synthesized[33]] at 5 °C and under N_2. The reaction mixture was stirred overnight at room temperature and then filtered, concentrated at reduced pressure, and chromatographed on silica gel (J. T. Baker Chemicals, 60−200 mesh) using $CHCl_3$ eluent. *N,N*-Bis(2-chloroethyl)-phosphoramidic diacid *O,O′*-bis(phenylmethyl) diester [$(ClCH_2CH_2)_2NP(O)(OCH_2C_6H_5)_2$] was obtained as an oil in 26% yield (2.6 mmol, 1.03 g, R_f 0.41): ^{1}H NMR (300 MHz, TMS/$CDCl_3$) δ 7.40−7.33 (m, 10 H, aromatic), 5.04 [d, $^3J_{HP} = 7.5$ Hz, 4H, two OCH_2], 3.55 [t, $^3J_{HH} = 7$ Hz, 4H, two CH_2Cl], and 3.37 [dt, $^3J_{HP} = 12$ Hz, $^3J_{HH} = 7$ Hz, 4H, two NCH_2]; ^{31}P NMR (121.49 MHz, $CDCl_3$) δ 9.1.

Pd/C (10%, 64 mg) and the diester synthesized above (1.3 mmol, 0.52 g) in CH_3OH (125 mL) were added to a three-neck round-bottomed flask equipped with a gas inlet (with stopcock) and a septum. Using the gas inlet, the flask was connected to a water aspirator and was degassed for 15 min. The stopcock was then closed and the flask was cooled to 5 °C. A balloon filled with H_2 and attached to a needle was then added to the reaction flask using the septum. The balloon was refilled as necessary to maintain a slight positive pressure of H_2. After 3 h of stirring at 5 °C, cyclohexylamine (5.1 mmol, 1.2 mL, 100% excess) was added and the reaction mixture was stirred at room temperature for 30 min. The mixture was then filtered and concentrated on a rotary evaporator at ambient temperature until the volume was reduced to ca. 15 mL. This solution was stored overnight at −20 °C; the resultant crystals were collected, washed with ether (3 × 4 mL), and dried under vacuum. *N,N*-Bis(2-chloroethyl)phosphoramidic diacid [$(ClCH_2CH_2)_2NP(O)(OH)_2$] as the dicyclohexylammonium salt was obtained as white crystals in 46% yield (0.6 mmol, 0.24 g): ^{1}H NMR [300 MHz, CD_3OD (HOD as reference set to δ 4.8)] δ 3.5−2.8 (multiplets, chloroethyl groups) [and for the cyclohexylammonium ion δ 2.0−1.9, 1.9−1.8, 1.7−1.6, and 1.5−1.1 (multiplets)]; ^{31}P NMR (CD_3OD) δ 4.1.

***N,N*-Bis(2-chloroethyl)phosphorodiamidic Acid (PM as the Free Acid).** *N,N*-Bis(2-chloroethyl)phosphorodiamidic acid phenylmethyl ester [$(ClCH_2CH_2)_2NP(O)NH_2(OCH_2C_6H_5)$] was synthesized according to literature procedures.[33] This benzyl ester (0.90 mmol, 0.27 g) was dissolved in CH_3OH (7 mL) and transferred to a three-neck round-bottomed flask containing 10% Pd/C (17 mg) and fitted with a gas inlet (with stopcock) and septa. The mixture was degassed for several minutes using a water aspirator attached to the flask through the gas inlet. The stopcock was then closed and the flask was

cooled to ca. 0 °C (NaCl/wet ice bath). A balloon filled with H_2 and attached to a needle was then added to the reaction flask through a septum. After 1 h of stirring at 0 °C under a slight positive pressure of H_2, the reaction mixture was filtered and the filtrate was concentrated at reduced pressure and ambient temperature to ca. 25% of its original volume. This solution was stored overnight at −20 °C; the resultant crystals were collected and washed with ether. Phosphoramide mustard was obtained as the free acid in 44% yield (85 mg, 0.4 mmol): ^{1}H NMR (D_2O) δ 3.67 [t, $^3J_{HH} = 7$ Hz, 4H, two CH_2Cl] and 3.36 [dt, $^3J_{HH} = 7$ Hz, $^3J_{HP} = 11$ Hz, 4H, two NCH_2]; ^{31}P NMR (D_2O) δ 9.4.

***N,N*-Bis(2-chloroethyl)phosphorodiamidic-^{3}*H* Acid Cyclohexylammonium Salt (PM-^{3}*H*).** Using unlabeled starting materials, *N,N*-bis(2-chloroethyl)phosphorodiamidic acid phenylmethyl ester [$(ClCH_2CH_2)_2NP(O)NH_2(OCH_2C_6H_5)$] was synthesized according to literature procedures.[33] This material was then randomly tritiated through a commercial source, SibTech, Inc. (Tenafly, NJ). All readily exchangeable labels were removed, and the material which was returned to us had an activity of 1.1 mCi/mg.

The solution from SibTech (15 mg of the tritiated benzyl ester in 1.5 mL of ethanol) was transferred to a test tube (with ethanol washings of original container) and to this was added unlabeled benzyl ester (35 mg). [The total benzyl ester used, then, was 50 mg or ca. 0.16 mmol.] The ethanol was evaporated under a stream of N_2, and the residue was dissolved in CH_3OH (several milliliters). This was evaporated under N_2, and then more CH_3OH was added and evaporated again (to remove all traces of ethanol). The residue was taken up in 0.7 mL of CH_3OH and transferred to a 25-mL, three-neck round-bottomed flask containing 10% Pd/C (3.3 mg). The test tube was washed with more CH_3OH (2 × 0.35 mL), and this also was added to the round-bottom flask. The flask was cooled to 5 °C (ice/water bath), and the contents were then degassed for several minutes using a gas inlet (with stopcock) connected to a water aspirator. The stopcock was then closed. A balloon filled with H_2 and attached to a needle was then added to the reaction flask using a septum. The flask was degassed a second time and then recharged with H_2 via a balloon. After 1 h of stirring at 5 °C under a slight positive pressure of H_2, the reaction mixture was filtered using CH_3OH washes. Cyclohexylamine (0.66 mmol, 76 μL) was added to the filtrate, and this was stirred at room temperature for 1 h. The solution was then concentrated at ambient temperature until the volume was reduced to ca. 1 mL. During storage overnight at −20 °C, crystals formed. The mother liquor was removed by pipet, and the crystals were washed with ether and dried using a water aspirator. *N,N*-Bis(2-chloroethyl)-phosphorodiamidic-^{3}*H* acid (PM-^{3}*H*) as the cyclohexylammonium salt was obtained as white crystals in ca. 44% yield (ca. 0.07 mmol, 22.3 mg), ^{31}P NMR (CD_3OD) δ 12.5. A small impurity (4% of total phosphorus intensity) was observed at δ 19.1. The activity of the product was 39 μCi/mg (ca. 13 μCi/μmol). (Note: The "loss" of activity, relative to starting benzyl ester, was due to the fact that in the labeling process tritium was first incorporated into the most reactive positions, those of the benzyl moiety. The mustard positions were more resistant to the labeling and thus became tritiated last. The benzyl group was subsequently removed during hydrogenation leading to a large drop in activity. This was a drawback to this synthetic pathway.)

HPLC Experiments with PM-^{3}*H*. PM-^{3}*H* (1 mM, 0.3 μCi/μmol) in 25 mM triethanolamine HCl buffer (pH 7.2) was incubated at 37 °C alone or in the presence of GSH (10 mM) or sodium thiosulfate (50 mM). Samples (20 μL) were removed at intervals and stored at −20 °C until analyzed (generally, ≤24 h). Chromatographic separations used an ABZ-Plus column (150 mm × 4.6 mm, Supelco, Bellefonte, PA) eluted with acetonitrile and a solution of 20 mM tetrabutylammonium hydrogen sulfate in 20 mM potassium phosphate (pH 7.0) at a flow rate of 1 mL/min. A linear gradient from 0 to 20% acetonitrile during 15 min was followed by 5 min elution at 20% acetonitrile. Sixty fractions of 0.33 min were collected. Each fraction was mixed with 1 mL scintillation fluor (Formula-963, Packard Instrument Co., Meriden, CT), and radioactivity was determined by scintillation counting.

The radioactivity in each fraction was expressed as a fraction of the total recovered radioactivity. Assignments of components of the chromatograms were based on considerations of kinetics, UV absorption (for glutathionylated species), literature reports of the same or similar compounds,[10,25] and cochromatography with authentic PM. Typical elution pattern on the reverse phase column [compound (fractions)]: bishydroxylated **10** (6−9); monohydroxylated **8** (19−23); bisglutathionylated **5** (24−28); monoglutathionylated **3** (33−37); PM (38−41); thiosulfate monoalkylated intermediate (48−52); and thiosulfate bisalkylated product (54−58). Note, ion pairing between the thiosulfate adducts and the tetrabutylammonium ion in the eluent reversed the polarity of these species.

Acknowledgment. We thank Dr. Vadappuram Chacko (Department of Radiology, Johns Hopkins University School of Medicine) for his generous assistance with many facets of the NMR work. We also thank Carol A. Hartke and Sung Y. Han (Oncology Center, Johns Hopkins University School of Medicine) for their contributions toward the synthesis of model and radiolabeled materials. Spectra for Figure 1 were obtained with the help of Dr. Tanya Dyakonov (Duke Comprehensive Cancer Center); we are grateful for her time and assistance. This work was supported in part by Public Health Service Grants 5-RO1-CA16783 (O.M.C.), CA51229 (M.P.G.), and CA09243-14 (training grant to E.M.S.-R.) from the National Cancer Institute (Department of Health and Human Services).

References

(1) Friedman, O. M.; Myles, A.; Colvin, M. Cyclophosphamide and Related Phosphoramide Mustards. Current Status and Future Prospects. *Adv. Cancer Chemother.* **1979**, *1*, 143−204.
(2) Stec, W. J. Cyclophosphamide and Its Congeners. *Organophosphorus Chem.* **1982**, *13*, 145−174.
(3) Colvin, M.; Chabner, B. A. Alkylating Agents. In *Cancer Chemotherapy: Principles and Practice*; Chabner, B. A., Collins, J. M., Eds.; J. L. Lippincott: Philadelphia, PA, 1991; pp 276−313.
(4) Colvin, O.; Friedman, H.; Gamcsik, M.; Fenselau, C.; Hilton, J. Role of Glutathione in Cellular Resistance to Alkylating Agents. *Adv. Enzyme Regul.* **1993**, *33*, 19−26.
(5) Colvin, O. M. Mechanisms of Resistance to Alkylating Agents. In *Anticancer Drug Resistance: Advances in Molecular and Clinical Research*; Goldstein, L. J., Ozols, R. R., Eds.; Kluwer Academic Publishers: Norwell, MA, 1994; pp 249−262.
(6) Yuan, Z.-M.; Smith, P. B.; Brundrett, R. B.; Colvin, M.; Fenselau, C. Glutathione Conjugation with Phosphoramide Mustard and Cyclophosphamide. A Mechanistic Study Using Tandem Mass Spectrometry. *Drug Metab. Disp.* **1991**, *19*, 625−629.
(7) Dirven, H. A. A. M.; Venekamp, J. C.; van Ommen, B.; van Bladeren, P. J. The Interaction of Glutathione with 4-Hydroxycyclophosphamide and Phosphoramide Mustard, Studied by ^{31}P Nuclear Magnetic Resonance Spectroscopy. *Chem.-Biol. Interact.* **1994**, *93*, 185−196.
(8) Engle, T. W.; Zon, G.; Egan, W. ^{31}P NMR Investigations of Phosphoramide Mustard: Evaluation of pH Control Over the Rate of Intramolecular Cyclization to an Aziridinium Ion and the Hydrolysis of This Reactive Alkylator. *J. Med. Chem.* **1979**, *22*, 897−899.
(9) Engle, T. W.; Zon, G.; Egan, W. ^{31}P NMR Kinetic Studies of the Intra- and Intermolecular Alkylation Chemistry of Phosphoramide Mustard and Cognate N-Phosphorylated Derivatives of *N,N*-Bis(2-chloroethyl)amine. *J. Med. Chem.* **1982**, *25*, 1347−1357.
(10) Watson, E.; Dea, P.; Chan, K. K. Kinetics of Phosphoramide Mustard Hydrolysis in Aqueous Solution. *J. Pharm. Sci.* **1985**, *74*, 1283−1292.
(11) Shulman-Roskes, E. M.; Noe, D.; Marlow, A.; Colvin, O. M.; Gamcsik, M. P.; Ludeman, S. M. Phosphoramide Mustard: Glutathione Alkylation vs P-N Bond Hydrolysis. *Proc. Am. Assoc. Cancer Res.* **1996**, *37*, 379 (no. 2590).
(12) Lu, H.; Chan, K. K. Gas Chromatographic-Mass Spectrometric Assay for N-2-Chloroethylaziridine, a Volatile Cytotoxic Metabolite of Cyclophosphamide, in Rat Plasma. *J. Chromatogr. B: Biomed. Appl.* **1996**, *678*, 219−225.

(13) Boal, J. H.; Williamson, M.; Boyd, V. L.; Ludeman, S. M.; Egan, W. ^{31}P NMR Studies of the Kinetics of Bisalkylation by Isophosphoramide Mustard: Comparisons with Phosphoramide Mustard. *J. Med. Chem.* **1989**, *32*, 1768−1773.
(14) Hehre, W. J.; Radom, L.; Schleyer, P.v. R.; Pople, J. A. *Ab Initio Molecular Orbital Theory*; Wiley-Interscience: New York, 1986.
(15) Szabo, A.; Ostlund, N. S. *Modern Quantum Chemistry Introduction to Advanced Electronic Structure Theory*; McGraw-Hill: New York, 1989.
(16) Dewar, J. S.; O'Connor, B. M. Testing Ab Initio Procedures: The 6-31G* Model. *Chem. Phys. Lett.* **1987**, *138*, 141−145.
(17) Millis, K. K.; Colvin, M. E.; Shulman-Roskes, E. M.; Ludeman, S. M.; Colvin, O. M.; Gamcsik, M. P. Comparison of the Protonation of Isophosphoramide Mustard and Phosphoramide Mustard. *J. Med. Chem.* **1995**, *38*, 2166−2175.
(18) Emsley, J.; Hall, D. *The Chemistry of Phosphorus*; John Wiley & Sons: New York, 1976; p 382.
(19) Rauen, H. M.; Norpoth, K. A Volatile Alkylating Agent in the Exhaled Air Following the Administration of Endoxan. *Klin. Wochenschr.* **1968**, *46*, 272−275.
(20) Gamcsik, M. P.; Ludeman, S. M.; Shulman-Roskes, E. M.; McLennan, I. J.; Colvin, M. E.; Colvin, O. M. Protonation of Phosphoramide Mustard and Other Phosphoramides. *J. Med. Chem.* **1993**, *36*, 3636−3645.
(21) Ludeman, S. M.; Zon, G.; Colvin, O. M.; Gamcsik, M. P.; Shulman-Roskes, E. M. NMR Spectroscopy and Drug Metabolism: Studies of Cyclophosphamide Metabolites. *Curr. Top. Med. Chem.* **1993**, *1*, 155−171.
(22) Colvin, M.; Brundrett, R. B.; Kan, M.-N. N.; Jardine, I.; Fenselau, C. Alkylating Properties of Phosphoramide Mustard. *Cancer Res.* **1976**, *36*, 1121−1126.
(23) Solomons, T. W. G. *Organic Chemistry, 4th ed.*; John Wiley & Sons: New York, 1988; p 886.
(24) Gamcsik, M. P.; Millis, K. K.; Hamill, T. G. Kinetics of the Conjugation of Aniline Mustards With Glutathione and Thiosulfate. *Chem.-Biol. Interact.* **1997**, *105*, 35−52.
(25) Bolton, M. G.; Hilton, J.; Robertson, K. D.; Streeper, R. T.; Colvin, O. M.; Noe, D. A. Kinetic Analysis of the Reaction of Melphalan with Water, Phosphate, and Glutathione. *Drug Metab. Disp.* **1993**, *21*, 986−996.
(26) Chan, K. K.; Hong, P. S.; Tutsch, K.; Trump, D. L. Clinical Pharmacokinetics of Cyclophosphamide and Metabolites with and without SR-2508. *Cancer Res.* **1994**, *54*, 6421−6429.
(27) Hong, P. S.; Srigritsanapol, A.; Chan, K. K. Pharmacokinetics of 4-Hydroxycyclophosphamide and Metabolites in the Rat. *Drug Metab. Disp.* **1991**, *19*, 1−7.
(28) Ludeman, S. M.; Ho, C.-K.; Boal, J. H.; Sweet, E. M.; Chang, Y. H. Carboxyphosphamide: NMR Studies of its Stability and Cell Membrane Permeability. *Drug Metab. Disp.* **1992**, *20*, 337−338.
(29) Jardine, I.; Fenselau, C.; Appler, M.; Kan, M.-N.; Brundrett, R. B.; Colvin, M. Quantitation by Gas Chromatography-Chemical Ionization Mass Spectrometry of Cyclophosphamide, Phosphoramide Mustard, and Nornitrogen Mustard in the Plasma and Urine of Patients Receiving Cyclophosphamide Therapy. *Cancer Res.* **1978**, *38*, 408−415.
(30) Boyd, V. L.; Robbins, J. D.; Egan, W.; Ludeman, S. M. ^{31}P Nuclear Magnetic Resonance Spectroscopic Observation of the Intracellular Transformations of Oncostatic Cyclophosphamide Metabolites. *J. Med. Chem.* **1986**, *29*, 1206−1210.
(31) Chan, K.K.; Zheng, J. J.; Wang, J. J.; Dea, P.; Muggia, F. M. Retention of Cytotoxicity of Phosphoramide Mustard (PM) Aqueous Solution After Its Complete Degradation. *Proc. Am. Assoc. Cancer Res.* **1994**, *35*, 300 (no. 1785).
(32) Gamcsik, M. P.; Hamill, T. G.; Colvin, M. NMR Studies of the Conjugation of Mechlorethamine with Glutathione. *J. Med. Chem.* **1990**, *33*, 1009−1014.
(33) Ludeman, S. M.; Shulman-Roskes, E. M.; Gamcsik, M. P.; Hamill, T. G.; Chang, Y. H.; Koo, K. I.; Colvin, O. M. Synthesis of ^{15}N and ^{17}O Labeled Phosphoramide Mustards. *J. Labelled Compd. Radiopharm.* **1993**, *33*, 313−326.

JM9704659